BUTTERWORTH HEINEMANN

Polymer Vol. 36 No. 8, pp. 1569–1575, 1995

0032-3861/95/$10.00 + 0.00

Morphologies of strongly segregated polystyrene–poly(dimethylsiloxane) diblock copolymers

Jennifer H. Chu*, Pratima Rangarajan, J. LaMonte Adams and Richard A. Register†

Department of Chemical Engineering, Princeton University, Princeton, NJ 08544, USA
(Received 1 August 1994)

Five polystyrene–poly(dimethylsiloxane) (PS/PDMS) diblocks were synthesized by sequential anionic polymerization, and their morphologies characterized by small-angle X-ray scattering (SAXS) and transmission electron microscopy (TEM). All materials are microphase-separated in toluene-cast films, and estimates of the interaction parameter χ indicate that these materials are all strongly segregated. The experimentally determined phase diagram is strongly skewed towards low styrene volume fractions, even more than the styrene–isoprene (SI) diblock phase diagram, even though little conformational asymmetry should exist in the PS/PDMS system. The PS/PDMS diblocks form substantially larger microdomain structures than the analogous SI diblocks, reflecting the stronger segregation strength.

(Keywords: diblock copolymer; polystyrene; poly(dimethylsiloxane))

INTRODUCTION

The synthesis of polystyrene–poly(dimethylsiloxane) (PS/PDMS) diblock copolymers was first reported 25 years ago[1–4]. Compared with conventional styrene–diene diblocks, the PS/PDMS system should have some unusual features, such as a very strong segregation between the two blocks and pronounced surface activity of the PDMS block[5,6], both of which result from the non-polar nature of PDMS. The resistance of siloxane-containing polymers to oxygen reactive ion etching also suggests potential uses for these diblocks in microlithography[7,8]. Surprisingly, no systematic investigation of the morphology of these materials has been undertaken, in contrast to the large body of work on the styrene–diene systems[9,10]. Saam and coworkers examined several PS/PDMS block copolymers by transmission electron microscopy (TEM), by casting thin films from toluene[1,2]. While these micrographs clearly indicate microphase separation, the images generally show disordered structures which are difficult to assign to the classical morphologies of spheres, cylinders, or lamellae. Moreover, it has since been shown that the presence of a surface can induce a morphological transformation when one block has a strong affinity for the surface[6,11], suggesting that the structure in thin cast films may not properly represent the bulk morphology. Cross-sectional TEM images shown by Chen *et al.*[6] of a PS/PDMS diblock with 22.5 wt% PS content reveal a lamellar morphology near the surface, while the bulk material exhibits cylinders of PS. Thus, the detailed phase diagram of the PS/PDMS system, i.e. which morphologies occur as the composition is varied, remains unknown. Here, we examine the bulk morphology of five PS/PDMS diblock copolymers with PS contents ranging from 9 to 69 wt%, and compare the observed morphologies and their characteristic domain size scales with the well studied styrene–diene diblock copolymers.

* Present address: Department of Chemical Engineering, University of Texas, Austin, TX 78712-1062, USA
† To whom correspondence should be addressed

EXPERIMENTAL

Diblock synthesis

The block copolymers were synthesized by the sequential anionic polymerization of styrene and hexamethylcyclotrisiloxane (D_3) in benzene under a nitrogen atmosphere, at a living-end concentration of 3–7 mM, using a combination of approaches from the various synthetic methods reported in the literature[1–4,7,12]. Benzene was distilled from oligostyryllithium; styrene (Aldrich, 99%) was purified by passing it through a column containing inhibitor-removal packing and neutral alumina. The solution of styrene in benzene was sparged with nitrogen to remove dissolved oxygen. The sec-butyllithium initiator (Aldrich, 1.3 M in cyclohexane) was added dropwise via a syringe until the orange colour of the styryllithium persisted, after which the calculated charge was added. The styrene was allowed to polymerize for 1 h while the reaction flask was heated to 60°C, after which a small aliquot of the polystyrene block was withdrawn and its polymerization terminated with methanol to enable analysis to be carried out.

Because D_3 does not polymerize in hydrocarbon solvents[1,13], a small charge (2–4 molecules per living end) of 2-methoxyethylether (diglyme; Aldrich, 99.5%, anhydrous) was then added via a syringe to the reaction

flask, turning the solution dark red. Diglyme was selected as the promoter because it is effective at low levels, and thus could be used as received. Subsequently, a small charge (1–5 molecules per living end) of D_3 (Hüls America, 95%, used as received) in freshly distilled benzene, sparged with nitrogen, was added via a syringe. This caused a rapid loss of colour, yielding a pale yellow solution[4]. Subsequently, the remaining charge of D_3 solution was added, followed by sufficient diglyme to bring its concentration to 5 vol%. This staged addition of diglyme and D_3 was used to minimize termination of the styryllithium living ends, which are more sensitive to O_2 than the silanolate ends.

To avoid possible broadening of the molecular-weight distribution as full conversion of D_3 was approached[13], the polymerizations were halted 75 min after the addition of the D_3, which produced approximately 50% D_3 conversion. The polymerizations were terminated with a tenfold excess of chlorotrimethylsilane (Aldrich, 98%, used as received). Upon termination, the solutions turned cloudy, presumably due to precipitated LiCl. The solutions were washed successively with saturated aqueous sodium bicarbonate until basic (to remove any HCl generated by the excess terminator), and then with deionized water until neutral[1,7]. The polymers were recovered by precipitation into methanol or ethanol, and were then air dried.

Homopolymer removal

Gel permeation chromatography (g.p.c.) traces of the reaction products always revealed the presence of some homopolystyrene (homoPS), corresponding to a terminated first block. In some cases, a broader peak corresponding to homoPDMS was observed as well, as has been reported previously[1,4]. Presumably the homoPDMS arises from the presence of trace water added with the D_3, which can act as a chain transfer agent. Identification of an impurity as either homoPS or homoPDMS was straightforward by g.p.c., since in toluene the two polymers have refractive index increments of opposite sign, and thus produce positive- or negative-going peaks on the g.p.c. output. Different fractionation procedures were used to remove these homopolymer impurities and isolate diblock copolymers free from contamination at the level detectable by g.p.c. To remove homoPS, the polymer was dissolved in dioxane and a 50/50 solution of methanol/water added until the solution turned cloudy[4]. The block copolymer and any homoPDMS formed a floating mass, while the homoPS remained dissolved. Removal of the homoPDMS was more difficult, and two different procedures were used. For homo PDMS of much lower molecular weight than the block copolymer, standard solvent/non-solvent fractionation using toluene/methanol was adequate. For polymer samples 17 and 59 (see below), which had homoPDMS impurities with molecular weights comparable to the diblock, this procedure was ineffective. Instead, the polymers were dissolved in bromobenzene and refrigerated at 5°C, which caused the solutions to turn cloudy; the solutions were centrifuged at 12°C until they separated into a (majority) clear lower layer (containing predominantly block copolymer) and a thin cloudy upper layer (containing predominantly homoPDMS)[1]. Following fractionation, all polymers were vacuum dried at 110°C.

Instrumental procedures

Gel permeation chromatography employed a 60 cm Polymer Laboratories PLgel Mixed C column and a Knauer refractive index detector; toluene was used as the solvent, at a rate of 1.0 ml min^{-1}. The column was calibrated with a series of narrow-distribution polystyrene standards. ^1H nuclear magnetic resonance (n.m.r.) spectra were acquired in $CDCl_3$ at 300 MHz using a General Electric QE300 spectrometer. Polymer compositions were determined from the ratios of the $Si-CH_3$ resonance to the aromatic resonances of polystyrene. Differential scanning calorimetry (d.s.c.) was performed on a Perkin–Elmer DSC-7 calibrated with indium and mercury. Samples were quenched from room temperature, or above, at the maximum cooling rate of the instrument (nominally 320°C min^{-1}), and then scanned at 10°C min^{-1}. In some cases, this process was repeated; data shown are from the first or second heating scans, with glass transition temperatures (T_gs) being reported as the midpoints[14].

Samples for small-angle X-ray scattering (SAXS) and transmission electron microscopy (TEM) experiments were prepared by casting the block copolymers from solution in toluene, a neutral solvent (see Discussion), and annealing the samples in vacuum overnight at 110–120°C. The polymers with high styrene contents were quite brittle, while those with low styrene contents were semi-solid, so continuous self-supporting films for SAXS could not be prepared. Instead, polymers were cast directly onto ASTM V4 mica sheets (Asheville-Schoonmaker Mica Co., Newport News, VA; 20–60 μm thick). The procedures used for the SAXS measurements have been reported previously[15]; briefly, an Anton–Paar compact Kratky camera and a Braun one-dimensional position-sensitive detector were employed, and data were desmeared for slit length using the experimentally measured slit weighting function and the iterative method of Lake[16]. All SAXS measurements were conducted at room temperature. The thicknesses of the supported films were difficult to measure, so all data are expressed on a relative intensity (I) scale, plotted against the scattering vector, $q = (4\pi/\lambda)\sin\theta$, where θ is half the scattering angle and λ is the X-ray wavelength. Both the mica and thermal density fluctuations produce a scattering background which is essentially independent of q over the angular range of interest; this contribution was determined by fitting the intensity at high q, and was then subtracted from the data.

For examination by TEM, a piece of sample 59 (see below), approximately 0.5 mm thick, was embedded in epoxy and sectioned at −120°C using a Reichert-Jung FC4E cryoultramicrotome with a Diatome Cryo-Dry 35° diamond knife. Difficulties in microtoming similar PS/PDMS diblocks have been reported previously[14]. No staining was necessary, as the silicon in the PDMS phase provides adequate contrast. Samples were examined in bright field conditions using a Philips 400 transmission electron microscope operating at 100 kV.

RESULTS

The compositions and molecular weights of the five diblock copolymers after the removal of homopolymer, as well as the molecular weight of the PS block sampled prior to the addition of D_3, are given in *Table 1*. Diblocks are simply designated by their weight percentage of

styrene. Molecular weights of 50 kg mol^{-1} were targeted; the actual weight-average molecular weights (M_ws) of the diblocks ranged from 41 to 74 kg mol^{-1}. The M_w/M_n values obtained by g.p.c. on the block copolymers should be considered as apparent polydispersities, since the refractive index increments of the two blocks are very different (of opposite sign, in fact); therefore, any compositional polydispersity will affect the apparent molecular weight polydispersity. It should be noted that the diblock polydispersity increases with the PDMS weight fraction, as would be expected if the PDMS blocks have a broader molecular weight distribution than the PS blocks. To determine the diblock molecular weight, the number-average molecular weight (M_n) of the first block was divided by the weight fraction of styrene, determined by ^{1}H n.m.r. spectroscopy, to yield M_n for the diblock, which was converted to M_w by using the apparent polydispersity.

These PS/PDMS diblocks are expected to be very strongly segregated due to the non-polar nature of the PDMS block. A rough estimate of the Flory interaction parameter χ can be obtained from the following[17]:

$$\chi=(v/RT)(\delta_{PS}-\delta_{PDMS})^2 \quad (1)$$

where the arbitrary reference volume v is conveniently selected as 100 cm^3 mol^{-1}, and the solubility parameters are approximately 15.4 and 18.6 (J cm^{-3})$^{0.5}$ for PDMS and PS, respectively[18]. At 100°C, near the glass transition temperature of PS, this yields $\chi \sim 0.3$, which is roughly five times the strength of interaction between the styrene and isoprene units[19]. With this value of χ, the polymers in *Table 1* have values of χN ranging from 130 to 260, where N is the number of reference volumes occupied by one mole of chains. Mean-field theory predicts that a $\chi N = 10.5$ is sufficient for a symmetric block copolymer to be segregated[20]; despite the crudeness of using solubility parameters to estimate χ, we conclude that our polymers should be quite strongly segregated, even at these moderate molecular weights. As a manifestation of this, small cracks which formed in films of sample 59 during drying were not healed by annealing at 120°C overnight. Comparison with the work of Krause *et al.*[14], who used d.s.c. to evaluate phase separation in PS/PDMS diblocks with a range of compositions and generally lower molecular weights, shows that our polymers do indeed have several times the minimum molecular weight required for phase separation.

Figure 1 shows the subambient portions of the d.s.c. traces of all of the five diblock copolymers, in which three principal features are evident: the PDMS glass transition near −125°C, a cold-crystallization exotherm for the PDMS phase near −90°C, and a PDMS melting endotherm near −40°C. The heat flow values have been normalized by the weight fraction of PDMS in each block copolymer. The areas of the melting endotherms are, in general, larger than those of the corresponding cold-crystallization exotherms, particularly for samples 59 and 69, which means that the glass transition measured for the PDMS phase corresponds to partially crystalline material. However, Krause *et al.*[14] have noted that crystallinity does not discernibly affect T_g for the PDMS

Table 1 Molecular characterization data for the diblock copolymers

Sample	Weight fraction of styrene	M_w of S block (g mol^{-1})	M_w/M_n of S block	M_w of diblock (g mol^{-1})	M_w/M_n of diblock
9	0.09	5700	1.08	68100	1.12
17	0.17	12000	1.06	73900	1.11
38	0.38	18200	1.09	47600	1.09
59	0.59	26500	1.06	45300	1.06
69	0.69	28400	1.06	41400	1.06

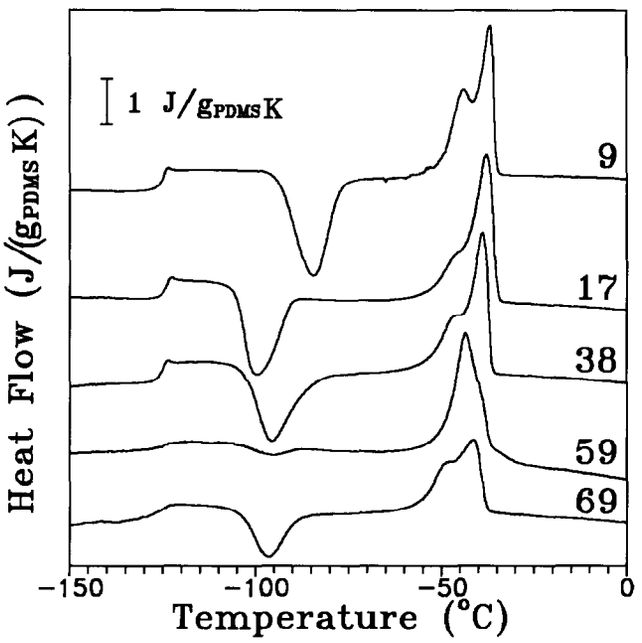

Figure 1 D.s.c. traces obtained for all five block copolymers; the heat flow scale has been normalized by the weight fraction of PDMS in each diblock

Table 2 Morphological characterization data for the diblock copolymers

Sample	Volume fraction of styrene (Φ_s)[a]	T_g of PDMS (PS) phase (°C)	Primary reflection q^* (nm^{-1})	Morphology	Microphase dimension (nm)[b]
9	0.08	−125.5	0.257	PS spheres	14.5
17	0.16	−124.5	0.140	PS cylinders	21.8
38	0.35	−125.5	0.127	Lamellae	24.7
59	0.56	−124.0	0.148	PDMS cylinders	33.9
69	0.66	−125.5(96)	0.175	PDMS cylinders	25.3

[a] At 100°C, calculated as described in text
[b] Sphere diameter (sample 9), cylinder diameter (samples 17, 59, 69), or half the lamellar repeat distance (sample 38)

phase, which is -125 ± 1°C for all five samples (see *Table 2*). The near constancy of the PDMS T_g across the five samples, which is also identical to the T_g of the PDMS homopolymer[14], demonstrates that all five polymers are microphase-separated, with no detectable phase mixing, as expected for strongly segregated materials. For those samples (9, 17, 38) which appear to have nearly amorphous PDMS phases at the glass transition, the change in heat capacity, ΔC_p, is 0.41–0.50 $J\,g_{PDMS}^{-1}\,K^{-1}$, in satisfactory agreement with Krause *et al.*[14]. The PS glass transition is substantially broader than that of PDMS in these block copolymers[14], and has a smaller value of ΔC_p, thus making it difficult to clearly discern this transition; for sample 69, the only one to exhibit a clear PS glass transition, the values of the T_g (96°C) and the normalized ΔC_p (0.31 $J\,g_{PS}^{-1}\,K^{-1}$) agree with the literature[14].

In interpreting the SAXS patterns for the PS/PDMS diblocks, we drew on the well documented SI diblock mesophase diagram, which has been summarized by Winey *et al.*[9]. (Unless specifically stated otherwise, we refer to SI diblocks wherein the isoprene block has a high content of 1, 4 units.) In the strong segregation limit, the boundaries separating one mesophase from another cease to be dependent on the molecular weight, and depend only on the composition for a given choice of monomers. To a first approximation, we might expect that SI diblocks and PS/PDMS diblocks of a similar PS volume fraction, Φ_S, would exhibit the same morphology. (As discussed below, this is *not* found in all cases.) To compute the values of Φ_S, the specific volumes of high-molecular-weight PS[21] and PDMS[22] at 100°C were estimated as 0.973 and 1.096 $cm^3\,g^{-1}$ respectively; 100°C, the glass transition temperature of polystyrene, was selected because any morphology present in the melt would be frozen in at this temperature upon cooling. Applying these specific volumes to the compositions determined by ^1H n.m.r. spectroscopy yielded the values of Φ_S listed in *Table 2*. In presenting the SAXS data, we have chosen to eliminate the influence of the form factor of the scattering entity at low q values by multiplying the intensity values by q for a cylindrical geometry and by q^2 for a lamellar geometry[23], where these corrections were appropriate.

SAXS and TEM were used to determine the morphology of each of the five block copolymers; the results are summarized in *Table 2*. The SAXS data for sample 9 are shown in *Figure 2*. The expected morphology of a material with this composition is PS spheres in a PDMS matrix[9]; the thin arrows denote calculated positions of the higher-order reflections, assuming the main peak at $q^* = 0.257\,nm^{-1}$ to be the 110 reflection of a body-centred cubic (bcc) lattice. Peaks at q-ratios of $1{:}\sqrt{2}{:}\sqrt{3}$ are clearly evident in *Figure 2*. Furthermore, the volume fraction Φ_S of PS (calculated at 100°C, but not strongly dependent on temperature) can be used to estimate the positions of the minima and maxima in the form factor for scattering from a single sphere (Rayleigh function)[24]; the maxima and minima are denoted by upward-pointing and downward-pointing bold arrows, respectively. Because these maxima are calculated from Φ_S, they are subject to errors from the determination of the PS weight fraction, as well as any deviations of the microphase mass densities from those of high-molecular-weight homopolymers; thus, they are best considered as estimates of where the form factor maxima and minima should lie, rather than precise calculations. For sample 9, these calculated positions are in satisfactory agreement with the observed maximum and minimum in the actual data, thus confirming the assignment of a bcc packing of PS spheres.

Figure 3 shows the SAXS data for sample 17, which would be expected to have a morphology of PS spheres or cylinders[24]. The arrows show the expected positions of peaks from a hexagonal lattice, assuming the main peak at $0.140\,nm^{-1}$ to be the 10 reflection; a peak at $\sqrt{3}$ is clearly evident, and a weak shoulder at $\sqrt{4}$ also

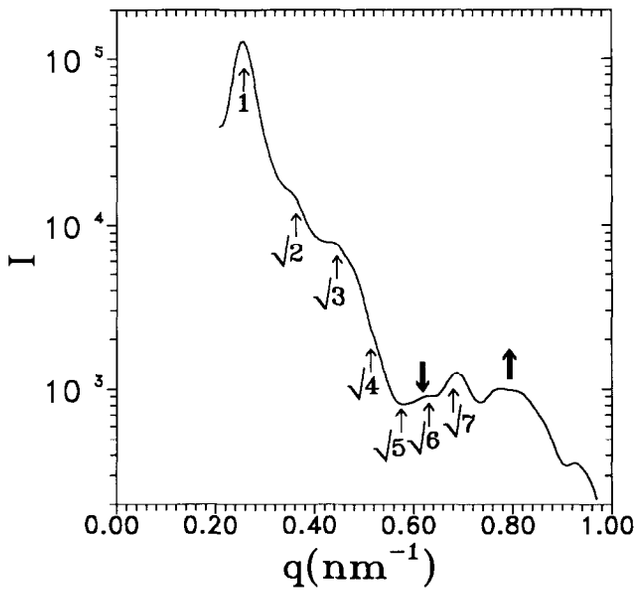

Figure 2 SAXS pattern for sample 9 ($\Phi_S = 0.08$). Thin arrows indicate the expected structure factor maxima for a bcc lattice; the bold downward arrow indicates the expected position of the form factor node for a sphere forming the appropriate volume fraction; the bold upward arrow indicates the expected position of the corresponding form factor maximum

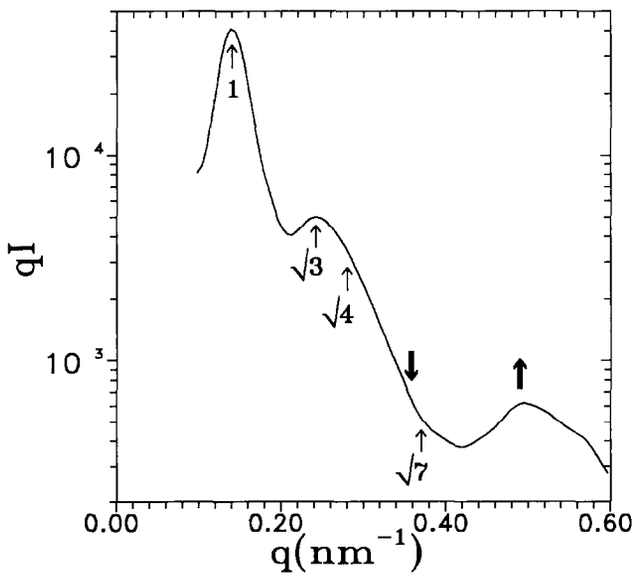

Figure 3 SAXS pattern for sample 17 ($\Phi_S = 0.16$). Thin arrows indicate the expected structure factor maxima for a two-dimensional hexagonal lattice; the bold downward arrow indicates the expected form factor node for a cylinder forming the appropriate volume fraction; the bold upward arrow indicates the expected position of the corresponding form factor maximum in this plot of qI vs. q

appears. The predicted form factor minima and maxima, for scattering from an isolated cylinder, are again consistent with the minimum and maximum observed in the data, confirming the assignment of PS cylinders. A similar analysis anticipating a spherical morphology shows poor agreement; in particular, the data are devoid of a discernible $\sqrt{2}$ peak, which would be predicted at a position far from any minimum in the form factor. It should be noted that the cylinder diameter determined from this analysis, i.e. 21.8 nm, is 37% *larger* than that found for an SI diblock of similar composition, but with a 16% *larger* molecular weight[24], suggesting that this PS/PDMS diblock forms a considerably larger microdomain structure than would an SI diblock of equal molecular weight.

Sample 38 would be expected to have a morphology of either PS cylinders, alternating lamellae, or perhaps a more complex cubic structure, such as the ordered bicontinuous double diamond[9] or the newly discovered gyroid structure[25]. The SAXS data (*Figure 4*) show peaks in a q-ratio of 1:2:3:4; as the volume fraction of PS in this polymer is ~ 0.35, the low intensity exhibited by the third-order peak is expected. Again, a similar analysis anticipating a cylindrical morphology, or a bicontinuous cubic phase, yields results inconsistent with the data. The lamellar repeat distance, i.e. 49.5 nm, is approximately 60% larger than that found in SI diblocks of a similar molecular weight, where the isoprene block is high in 3,4 content[26]. We have also studied[27] a SI diblock with a high 1,4 content and a molecular weight which is 9% below that of sample 38, and found a lamellar repeat distance of 28.6 nm, essentially the same value as for a corresponding SI diblock with a high 3,4 content[26]. Thus sample 38 also forms a substantially larger microdomain structure than a comparable SI diblock material.

Figure 5 shows SAXS data for sample 59, which again might exhibit lamellae, a bicontinuous cubic structure, or PDMS cylinders[9]. The scattering data are presented in anticipation of a cylindrical morphology; the calculated position of the form-factor minimum is close to the $\sqrt{3}$ reflection, which explains its absence. However, the

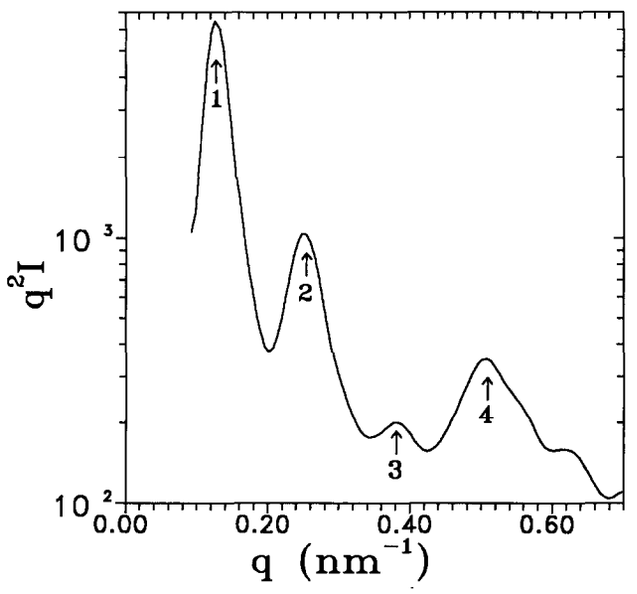

Figure 4 SAXS pattern for sample 38 ($\Phi_S = 0.35$). Thin arrows indicate the expected structure factor maxima for a one-dimensional lamellar stack

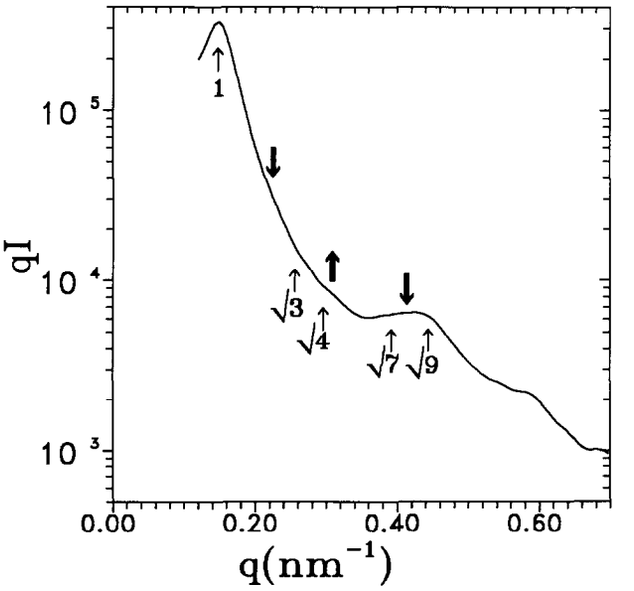

Figure 5 SAXS pattern for sample 59 ($\Phi_S = 0.56$). Arrows have the same meanings as in *Figure 3*

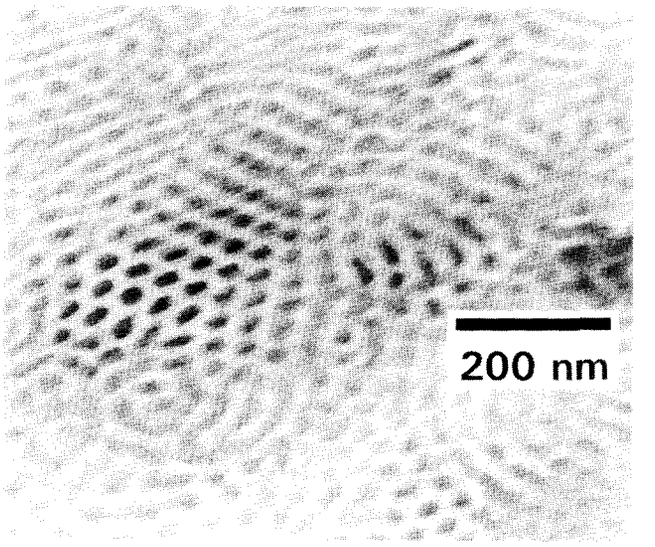

Figure 6 Bright-field transmission electron microscope image of sample 59. PDMS domains appear dark, and cylinders whose axes make various angles with the film plane are evident

SAXS data show only two clear peaks (marked as 1 and $\sqrt{9}$ in *Figure 5*), and are thus equally consistent with a lamellar morphology. For this sample, then, morphological confirmation by TEM was essential. *Figure 6* clearly shows that the morphology consists of PDMS cylinders (which appear dark in the micrograph) in a matrix of PS. The cylinder diameters are approximately 30 nm, in good agreement with the value of 33.9 nm determined from the position of the primary reflection in *Figure 5* and Φ_S. The grain size appears quite small in *Figure 6*, which may contribute to the indistinctness of the SAXS pattern.

Given that sample 59 exhibits a morphology of PDMS cylinders, the same was expected for sample 69. The SAXS data (*Figure 7*) show a weak reflection near $\sqrt{4}$ and a stronger peak at $\sqrt{7}$, consistent with a cylindrical morphology. The calculated position of the form factor minimum coincides with the expected $\sqrt{3}$ peak, thus

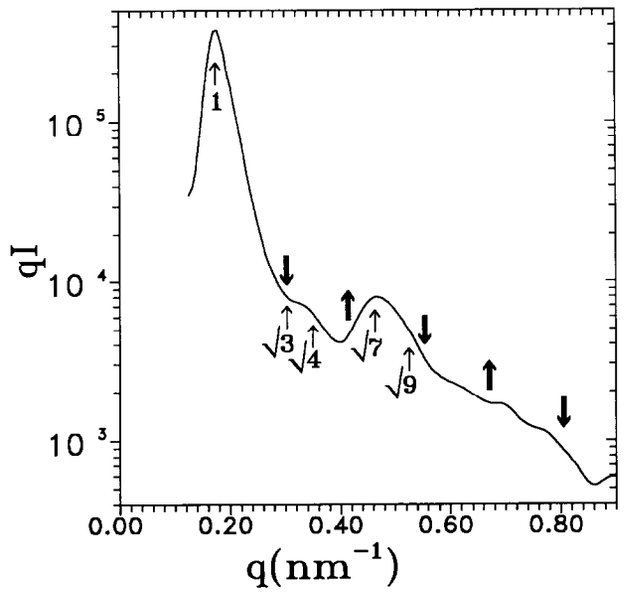

Figure 7 SAXS pattern for sample 69 ($\Phi_S = 0.66$). Arrows have the same meanings as in *Figure 3*

explaining its absence. Hashimoto *et al.*[28] have recently published calculations for hexagonally packed cylinders with paracrystalline distortion; for a PDMS volume fraction corresponding to sample 69, the relative prominences of the 1, $\sqrt{3}$, $\sqrt{4}$, $\sqrt{7}$, and $\sqrt{9}$ reflections are calculated to be very similar to those shown in *Figure 7*. An analysis assuming a morphology of PDMS spheres yields poor agreement with the data.

DISCUSSION

It is well known that the phase diagram of the SI system is asymmetric, with the order–order boundaries skewed towards the low volume fraction of polystyrene[9]. As an example, a SI diblock containing 20 vol% PS forms PS cylinders, while one containing 20 vol% PI forms PI spheres. This asymmetry is due to differences in the statistical segment length and density of the two blocks[29,30]. Our experimental results indicate that the PS/PDMS phase diagram is skewed even more than that obtained for SI diblocks, in the same direction. Sample 17, which would have a morphology of PS spheres in a SI diblock of equivalent volume fraction[9,24], has a morphology of PS cylinders; sample 59, which would have a lamellar morphology[9] in an equivalent SI diblock, contains PDMS cylinders, while sample 69, whose volume fraction would put it on the borderline between bicontinuous cubic and cylindrical structures in SI diblocks[9], is evidently well into the region where PDMS cylinders are preferred. Recently, Vavasour and Whitmore[30] have developed a self-consistent field theory which allows for asymmetry in the polymer statistical segment lengths, a factor which can substantially shift the boundaries between ordered phases. The asymmetry is captured in a parameter ε, which is defined as follows:

$$\varepsilon = \frac{v_A}{v_B}\left(\frac{R_{g,B}/M_B^{0.5}}{R_{g,A}/M_A^{0.5}}\right)^2 \qquad (2)$$

where v_i represent the specific volumes of the two blocks A and B, and the radii of gyration $R_{g,i}$ correspond to the unperturbed dimensions of the two blocks, as would be obtained from small-angle neutron scattering in the melt. From literature data, we estimate $R_g/M^{0.5}$ at 100°C to be 0.267 and 0.278 Å $mol^{0.5}\,g^{-0.5}$ for PS[31,32] and PDMS[33,34], respectively. Denoting PDMS as the A block yields $\varepsilon = 1.04$, suggesting that very little conformational asymmetry should exist in this polymer and that the phase diagram should be symmetrical. Although the uncertainty in this calculation of ε is substantial, principally due to variances among reported values for unperturbed dimensions, no combination of any of the R_g values found in the literature produced an ε value sufficiently small ($\varepsilon < 0.6$ would be required) for agreement with the experimental phase diagram.

Because these polymers are so strongly segregated, it is impossible to prepare a sample by quenching from a disordered melt, making it difficult to be certain that the morphologies obtained are equilibrium ones. The SAXS and TEM examinations were all on films cast from toluene (a solvent thought to be equally good for both blocks) in order to approach the equilibrium morphology as closely as possible. The Mark–Houwink exponents of 0.73 for PS[35] and 0.72 for PDMS[36] have been reported in toluene at 25°C, which indicates that toluene should be a non-selective, good solvent for PS/PDMS. However, if toluene were in fact slightly preferential towards PS, this could skew the phase boundaries in the observed direction[37,38]. In fact, the intrinsic viscosities $[\eta]$ calculated using the literature expressions[35,36] indicate that $[\eta]$ is approximately 40% larger for PS than for PDMS at the relevant molecular weights. However, the $[\eta]$ values of PS and polyisoprene differ by nearly a factor of 2 in toluene[39], and toluene is still considered to be a neutral solvent for SI diblocks, producing the equilibrium morphology in cast films[9,10,24], even for very high molecular weights (i.e. of comparable segregation strength to the PS/PDMS diblocks studied here). Thus, we are reluctant to attribute the asymmetry of the experimental phase diagram to selective solvent effects.

Where comparisons could be made (particularly for samples 17 and 38), it was noted that the PS/PDMS diblocks studied here form microdomain structures substantially larger than those produced by SI diblocks of similar molecular weight and composition. Although the statistical segment lengths and densities of the two blocks also influence the microdomain size scale, the prediction in the strong segregation limit[40] is that the domain size scales as $\chi^{1/6}N^{2/3}$. Therefore, a large increase in χ is expected to produce an increase in the domain spacing. It is difficult to quantitatively test this predicted χ dependence experimentally because of the difficulty in adjusting χ (through temperature, for example) while keeping all other material parameters (statistical segment length, density, etc.) constant. Nonetheless, a qualitative check of the prediction can be made by comparing two block copolymers which are so different in χ that this effect dominates.

Assuming that the $N^{2/3}$ scaling holds[26], then samples 17 and 38 have morphologies with characteristic dimensions which are 50–60% larger than those of the comparable SI diblocks. Unfortunately, comparisons for the other samples were difficult to make. A styrene–butadiene (SB) diblock, of similar composition to sample

9 and nearly twice the molecular weight, has been studied[41]; assuming a $N^{2/3}$ scaling, the domain sizes in the two polymers are comparable. However, it is well known that materials with a spherical morphology have great difficulty in achieving their equilibrium domain size during solvent evaporation, because of the discontinuous interfaces; as a result, domain sizes substantially below the equilibrium size are typically found[42]. Since our polymers are more strongly segregated than this SB diblock, the non-equilibrium effects may be expected to be more severe also, and a direct comparison is probably not valid. No comparison could be made for sample 59, since the SI and SB diblocks of this composition exhibit a lamellar, rather than a cylindrical, morphology. As regards sample 69, no comprehensive studies of SI diblocks containing I cylinders could be found in the literature. Comparison with the single polymer of this morphology ($\Phi_S = 0.76$) examined by Winey *et al.*[9], again assuming the $N^{2/3}$ scaling, indicates that the PS/PDMS system forms microdomains which are 36% larger. Although the exact factor is subject to some uncertainty, it appears that PS/PDMS diblocks form substantially larger microdomain structures than do the comparable styrene–diene polymers, which we believe reflects the considerably larger χ between the PS and PDMS repeat units.

CONCLUSIONS

The strongly segregated PS/PDMS block copolymers examined here exhibited morphologies which were well known from previous work on conventional styrene–diene diblocks, i.e. spheres, cylinders, and lamellae. However, the mesophase diagram is quite asymmetric, being skewed in the direction of low styrene content. This is not expected based on current theories incorporating statistical segment length asymmetry, coupled with literature values of statistical segment length and density. Although films were necessarily cast from solution, based on the intrinsic viscosities of homopolymers, toluene should be an essentially neutral solvent and thus produce the equilibrium morphology. Where comparisons could be made, the domain size scales found for these PS/PDMS diblocks were substantially greater (40–60%) than SI diblocks of similar composition and molecular weight, reflecting the significantly larger χ in the PS/PDMS system.

ACKNOWLEDGEMENTS

Support for this work was provided by Hoechst-Celanese Corporation, and by the National Science Foundation, Polymers Program (DMR-9257565) and Materials Research Group (DMR-9223966). The assistance of Joseph Goodhouse and Nan Yao (Princeton University) in preparing and examining sample 59 by TEM is gratefully acknowledged.

REFERENCES

1 Saam, J. C., Gordon, D. J. and Lindsey, S. *Macromolecules* 1970, **3**, 1
2 Saam, J. C. and Fearon, F. W. G. *Ind. Eng. Chem. Prod. Res. Dev.* 1971, **10**, 10
3 Davies, W. G. and Jones, D. P. *Ind. Eng. Chem. Prod. Res. Dev.* 1971, **10**, 168
4 Zilliox, J. G., Roovers, J. E. L. and Bywater, S. *Macromolecules* 1975, **8**, 573
5 Chen, X., Gardella, J. A. and Kumler, P. L. *Macromolecules* 1992, **25**, 6621
6 Chen, X., Gardella, J. A. and Kumler, P. L. *Macromolecules* 1992, **25**, 6631
7 Hartney, M. A., Novembre, A. E. and Bates, F. S. *J. Vac. Sci. Technol. B* 1985, **3**, 1346
8 DeSimone, J. M., York, G. A., McGrath, J. E., Gozdz, A. S. and Bowden, M. J. *Macromolecules* 1991, **24**, 5330
9 Winey, K. I., Gobran, D. A., Xu, Z., Fetters, L. J. and Thomas, E. L. *Macromolecules* 1994, **27**, 2392
10 Hasegawa, H., Tanaka, H., Yamasaki, K. and Hashimoto, T. *Macromolecules* 1987, **20**, 1651
11 Liu, Y., Zhao, W., Zheng, X., King, A., Singh, A., Rcfailovich, M. H., Sokolov, J., Dai, K. H., Kramer, E. J., Schwarz, S. A., Gebizlioglu, O. and Sinha, S. K. *Macromolecules* 1994, **27**, 4000
12 Yin, R. and Hogen-Esch, T. E. *Am. Chem. Soc. Div. Polym. Chem. Polym. Prepr.* 1992, **33**, 239
13 Yilgör, I. and McGrath, J. E. *Adv. Polym. Sci.* 1988, **86**, 1
14 Krause, S., Iskandar, M. and Iqbal, M. *Macromolecules* 1982, **15**, 105
15 Register, R. A. and Bell, T. R. *J. Polym. Sci. Polym. Phys. Edn* 1992, **30**, 569
16 Lake, J. A. *Acta Crystallogr.* 1967, **23**, 191
17 Bristow, G. M. and Watson, W. F. *Trans. Faraday Soc.* 1958, **54**, 1731
18 'Polymer Handbook' (Eds J. Brandrup and E. H. Immergut), 3rd Edn, Wiley, New York, 1989, p. VII/557
19 Adams, J. L., Graessley, W. W. and Register, R. A. *Macromolecules* 1994, **27**, 6026
20 Leibler, L. *Macromolecules* 1980, **13**, 1602
21 Richardson, M. J. and Savill, N. G. *Polymer* 1977, **18**, 3
22 'Silicon Compounds: Register and Review', 5th Edn, Hüls America, Inc., Piscataway, NJ, 1991, p. 254
23 Russell, T. P. in 'Handbook on Synchrotron Radiation' (Eds G. S. Brown and D. E. Moncton), Vol. 3, North-Holland, New York, 1991, p. 379
24 Sakurai, S., Kawada, H., Hashimoto, T. and Fetters, L. J. *Macromolecules* 1993, **26**, 5796
25 Hajduk, D. A., Harper, P. E., Gruner, S. M., Honeker, C. C., Kim, G., Thomas, E. L. and Fetters, L. J. *Macromolecules* 1994, **27**, 4063
26 Hashimoto, T., Shibayama, M. and Kawai, H. *Macromolecules* 1980, **13**, 1237
27 Rangarajan, P. and Register, R. A., unpublished results
28 Hashimoto, T., Kawamura, T., Harada, M. and Tanaka, H. *Macromolecules* 1994, **27**, 3063
29 Helfand, E. and Wasserman, Z. R. in 'Developments in Block Copolymers—1' (Ed. I. Goodman), Applied Science, New York, 1982, p. 99
30 Vavasour, J. D. and Whitmore, M. D. *Macromolecules* 1993, **26**, 7070
31 Tangari, C., King, J. S. and Summerfield, G. C. *Macromolecules* 1982, **15**, 132
32 Fetters, L. J., Lohse, D. J., Richter, D., Witten, T. A. and Zirkel, A. *Macromolecules* 1994, **27**, 4639
33 Beltzung, M., Picot, C., Rempp, P. and Herz, J. *Macromolecules* 1982, **15**, 1594
34 Mark, J. E. and Flory, P. J. *J. Am. Chem. Soc.* 1964, **86**, 138
35 Breitenbach, J. W., Gabler, H. and Olaj, O. F. *Makromol. Chem.* 1965, **81**, 32
36 Haug, A. and Meyerhoff, G. *Makromol. Chem.* 1962, **53**, 91
37 Beamish, A., Goldberg, R. A. and Hourston, D. J. *Polymer* 1977, **18**, 49
38 Bates, F. S. and Cohen, R. E. *J. Polym. Sci. Polym. Phys. Edn* 1980, **18**, 2143
39 Prud'homme, J., Roovers, J. E. L. and Bywater, S. *Eur. Polym. J.* 1972, **8**, 901
40 Semenov, A. N. *Sov. Phys. JETP* 1985, **61**, 733
41 Thomas, E. L., Kinning, D. J., Alward, D. B. and Henkee, C. S. *Macromolecules* 1987, **20**, 2934
42 Hashimoto, T., Fujimura, M. and Kawai, H. *Macromolecules* 1980, **13**, 1660